MEMS Viscosity Sensor

Arthur Ballato
US Army Communications-Electronics RDEC
Fort Monmouth, NJ 07703-5201, USA
a.ballato@IEEE.org

***Abstract*—Quartz shear resonators are employed widely as sensors to measure Newtonian viscosities of liquids. Perturbation of the electrical equivalent circuit parameters of the plate resonator by the fluid loading permits calculation of the mass density – shear viscosity product. Use of doubly rotated resonators does permit additional information to be obtained, but in no case can the viscosity and mass density values be separated. In these measurements, the resonator surface is exposed to a measurand bath whose extent greatly exceeds the penetration depth of the evanescent shear mode excited by the active element. Here we discuss the more complicated situation where the separation between the resonator and a confining wall is less than the penetration depth of the fluid occupying the intervening region. The resonator perturbation in this case is a sensitive function of the separation. This important fact permits extreme miniaturization, since for temperatures and pressures ordinarily encountered with gases and liquids, and for frequencies between 10 MHz and 1 GHz, the penetration depth varies from micrometers to nanometers. Micro-electro-mechanical (MEMS) versions of viscometers and associated types of fluid sensors are thereby enabled.**

I. INTRODUCTION

Quimby originated the technique of measuring solids by attaching them to a quartz crystal [1]. The Quimby composite resonator (QCR) reduces to that of the quartz crystal microbalance (QCM) [2-4] in the limit where the measurand becomes a thin film, and its elasticity is neglected [5-7]. Mason first adapted the technique for measuring liquids [8-10]. This method remains very popular, e.g., [11-18]. References [7,14] contain many more pertinent citations. Stockbridge used the modality to measure gases [19-20]. In these applications, the crystal resonator is measured without, and then with, the loading of the measurand. Ensuing changes are registered as changes in frequency, phase, and/or impedance level, from which the unknown measurand properties are inferred.

II. EQUIVALENT ELECTRIC NETWORK

Over the years, many equivalent circuits have been used to model the piezoresonator, and to describe its behavior when its surface is subjected to various conditions of loading [21-25]. The most popular is the Butterworth–Van Dyke (BVD) network, consisting of a capacitance C_0, shunted by an R_1, L_1, and C_1 series arm [21]. The series arm is the manifestation of the piezoelectrically induced vibratory motion at a single isolated resonance. The BVD lumped circuit evolved into more elaborate broad-band, multi-mode, transmission-line networks that place the mechanical boundary loadings and piezoelectric excitation mechanism in series at the surfaces [23-24].

III. FLUID LOADING

We consider one surface of the piezoelectric resonator to be in contact with a fluid to be measured. Lord Rayleigh, commenting on Stokes' treatment of fluid viscosity, wrote [26, §347]: "The velocity of the fluid in contact with the plane is usually assumed to be the same as that of the plane itself on the apparently sufficient ground that the contrary would imply an infinitely greater smoothness of the fluid with respect to the solid than with respect to itself." This assumption is implicit in the following treatment.

An unbounded Newtonian fluid, (i.e., a fluid with shear viscosity, η, in addition to the usual attributes of mass density, ρ, and elastic stiffness c_L), in intimate contact with a resonator surface of area A, presents to the surface both shear (S) and longitudinal (L) impedances. These depend on angular frequency, ω. Mechanical shear impedance is $Z_S = A\sqrt{(j\omega\eta\rho)} = R_S + j\omega L_S$. R_S represents shear dissipation, and L_S models entrained mass loading. Penetration depth is $\delta = \lambda/2\pi = \sqrt{(2\eta/\rho\omega)}$. Longitudinal impedance consists of $R_L = A\rho v_L = A\sqrt{(\rho c_L)}$, representing energy radiating into the fluid, plus a small reactance representing wave attenuation; we neglect longitudinal viscosity. These impedances, transformed by a piezoelectric factor, appear in the BVD circuit in series with the R_1, L_1, C_1 branch [16-17]. Thus, immittance and/or frequency measurements on a resonator immersed in an unbounded fluid (i.e., when distance (ℓ) from the resonator surface to a confining surface greatly exceeds the penetration depth, δ), yield only the (ρc_L) and ($\eta\rho$) products. The BVD representation of a resonator in an unconfined fluid is depicted in Fig. 1.

IV. CONFINED FLUID LOADING

For the great majority of fluids and ambient conditions and frequencies of interest, the penetration depth, δ, characterizing the evanescent shear wave, ranges from micrometers to nanometers. We consider the effect of introducing a planar rigid boundary parallel to the surface of the piezoelectric resonator in order to confine the fluid therebetween. Fine adjustments to the spacing between the surfaces are easily accommodated by the use of a second piezoelectric element, or, e.g., an "inchworm" mechanism [27].

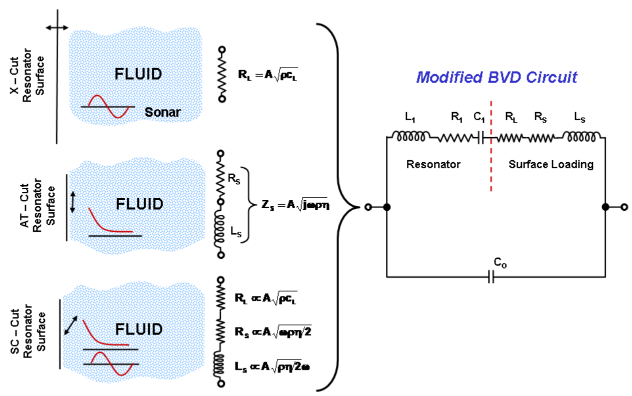

Figure 1. BVD representation of resonator in unconfined fluid.

When the distance, ℓ, separating the two surfaces becomes comparable to δ, the formulas above no longer hold. Instead, the surface of the resonator sees a complex mechanical admittance of (see Figs. 2 and 3)

$$A\cdot Y_S = A\cdot(G_S + jB_S) = \sqrt{(j/2)}\cdot(\delta/\eta)\cdot\tan[\sqrt{(2/j)}\cdot(\ell/\delta)]. \quad (1)$$

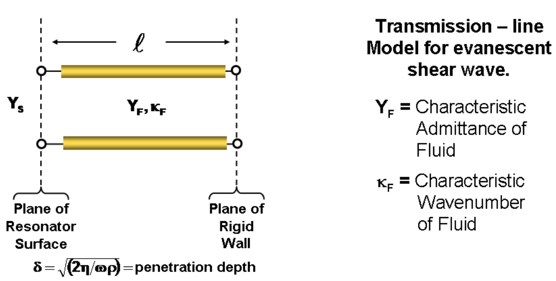

Figure 2. Input admittance of confined evanescent shear wave.

The complex mechanical impedance is

$$Z_S = R_S + jX_S = 1/Y_S. \quad (2)$$

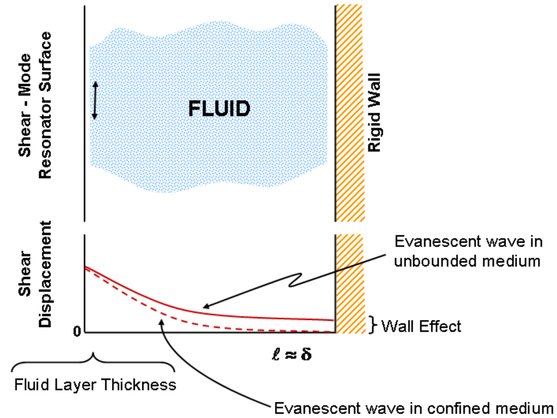

Figure 3. Effect of rigid wall on evanescent shear wave.

With the abbreviations w = (ℓ/δ) and p = (δ/η), shear conductance, $G_S(w)$ and reactance $X_S(w)$ are:

$$G_S = g(w)\cdot(p/A) = g(w)/[A\cdot\sqrt{(\omega\rho\eta/2)}], \quad (3)$$

$$X_S = x(w)\cdot(A/p) = x(w)\cdot A\cdot\sqrt{(\omega\rho\eta/2)}, \text{ where} \quad (4)$$

g(w) and x(w) are dimensionless factors with the general form of a tanh function with superposed cyclic modulation. When a second resonator, driven at the same frequency, replaces the stationary wall, the phase angle (ϕ) between the two resonator surfaces can be used as another means of measurement. Then the dimensionless factors g , w, etc., also depend on ϕ. Figures 4 and 5 show g(w,ϕ) and x(w, ϕ), respectively. The first three extrema of g(w.0) are 0.68111 at w = 0.9375, 0.49093 at w = 2.347 and 0.50039 at w = 3.929; g(0,0) = 0, and g(∞,0) = 1/2. The first extremum of x(w,0) is 1.0178 at w = 2.366; x(0,0) = 0, and x(∞,0) = 1. At w = 0, the slopes are: dg(0,0)/dw = +1, and dx(0,0)/dw = +2/3. Similarly defined factors, b(w, ϕ), |y(w, ϕ)|, r(w, ϕ), |z(w, ϕ)| behave as follows for w << 1: r(w,0) and |z(w,0)| are hyperbolic; |y(w,0)| is linear, and b(w,0) is zero, with zero slope.

V. Viscosity and Mass Density

When w << 1, g(w,0) ≈ [dg(w,0)/dw]·w ≈ w = (ℓ/δ), and viscosity η may be determined directly from the relation

$$A\cdot\eta = (\Delta G_S/\Delta\ell)^{-1} \quad (5)$$

Similarly,

$$A\cdot\rho = (3/\omega)\cdot(\Delta X_S/\Delta\ell). \quad (6)$$

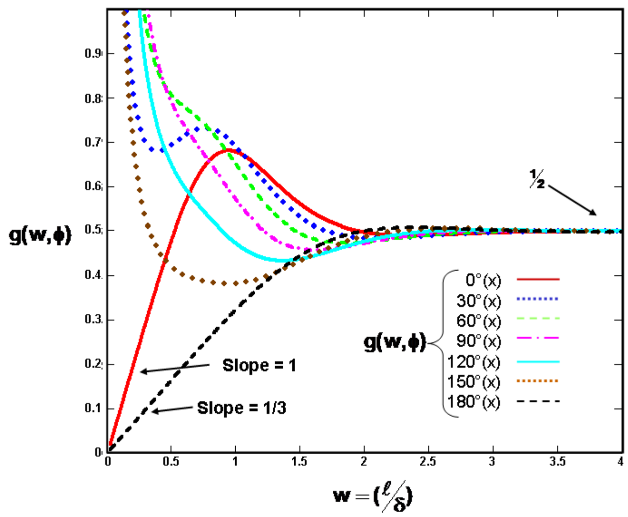

Figure. 4 Mechanical conductance function g(w,ϕ).

Equations (5) and (6) express mechanical values. In order to convert them to electrical form, G_S is multiplied, and X_S is divided, by the factor $n^2 = (Ae/t)^2$, where e is an effective piezoelectric stress coefficient, and t the thickness of the resonator.

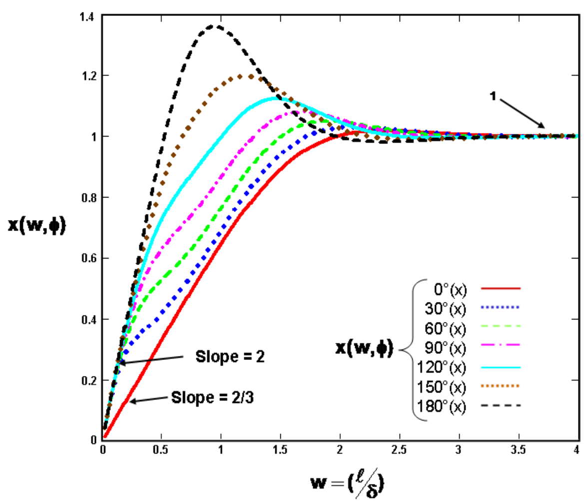

Figure. 5 Mechanical reactance function x(w,ϕ).

Thus, for w in the range where g(w, ϕ) and x(w, ϕ) are linear, automatic network analyzer measurements yield direct determinations of viscosity and mass density. As a check, the region w >> 1 provides the (ρη) product. Similar remarks pertain to use of longitudinal resonators to yield values of the compressional stiffness (c_L) directly. Because δ is usually very small, MEMS miniaturization is a natural consequence of using the w << 1 regime.

VI. Numerical Values

Rayleigh [26, p.313] remarks: "Both by theory and experiment the remarkable conclusion has been established that within wide limits the force *[viscosity]* is independent of the density of the gas." Tables 1 and 2 contain values of pertinent acoustic properties of CO_2 at 300 and 400K, and N_2 at 200 and 400K, [28,29]. In these tables and those below, the δ values are for a frequency of 1 MHz. R_S is the mechanical resistance; units are kg/(s·m^2).

A useful expression for δ is as follows, where viscosity is in units of milli-pascal-seconds, mass density is in Mg/m^3 and frequency is in MHz:

$$\delta = 0.399 \sqrt{[\eta/(\rho f]}. \quad (7)$$

Pressure	R_S	δ	R_S	δ
atm		μm		μm
0.01	0.916	16.31	0.902	21.41
0.1	2.898	5.158	2.853	6.772
1	9.186	1.627	9.029	2.140
10	29.75	0.503	28.79	0.671
100			99.90	0.1934
T →	300 K		400 K	

Table 1 - Acoustic parameters of CO_2

Pressure	R_S	δ	R_S	δ
atm		μm		μm
0.01	0.8330	15.54	0.7680	28.63
0.1	2.636	4.914	2.429	9.057
1	8.343	1.552	7.679	2.864
10	26.64	0.4862	24.31	0.909
100	90.70	0.1428	77.50	0.3001
T →	200 K		400 K	

Table 2 - Acoustic parameters of N_2

Tables 3 and 4 provide acoustic values for additional fluids. When dealing with miniaturized devices having fluid gaps in the order of micrometers to nanometers, one must take into account the deviations from Newtonian behavior due to finite atomic and molecular dimensions of the fluids. In addition, for gases at pressures below about ½ atm, viscoelastic behavior [19] is observed, and one must deal with a complex viscosity having a relaxation frequency (Maxwell fluid); see also [14]. Data are from [25,29-31].

Substance	ρ	η	δ	Rs
	kg/m^3	mPa-s	μm	
Hexane	660.6	0.3	0.380	0.789
Heptane	679.5	0.387	0.426	0.909
Octane	698.6	0.508	0.481	1.056
Nonane	719.2	0.665	0.543	1.226
Decane	726.6	0.838	0.606	1.383
Dodecane	749.5	1.383	0.766	1.805
Cyclohexane	773.9	0.894	0.606	1.474
Octanol	826.2	7.288	1.676	4.349
Hexanol	813.6	4.578	1.338	3.421
Isopropanol	780.9	2.038	0.911	2.236

Table 3 Parameters of alkanes and alcohols at RT. Rs has units here of Mg/(s·m^2)

Substance	T_m	ρ_m	η_m	δ
	°C	Mg/m^3	mPa-s	μm
GaSb	706.	6.03	1.00	0.162
GaAs	1238.	5.71	4.0	0.334
InSb	525.	6.48	2.34	0.240
InP	1062.	6.03	0.801	0.145

Table 4 Acoustic parameters of molten binaries

VII. CONCLUSION

We have considered Newtonian fluids subjected to shear motion, in the limit where the distance to a confining rigid wall is comparable to the penetration depth. It is found that the immittance seen at the face of the shear transducer, (and reflected in the transducer equivalent electrical circuit values), permits direct determination separately of the viscosity and mass density. The smallness of the penetration depth, in most applications, is such to enable extreme miniaturization.

REFERENCES

[1] S. L. Quimby, "On the experimental determination of the viscosity of vibrating solids," Phys. Rev. 25, 558-573 (1925)

[2] G. Sauerbrey, "Wägung dünner Schichten mit Schwingquarzen," Physikalische Verhandlungen, 8, 193 (1957)

[3] G. Sauerbrey, "Verwendung von Schwingquarzen zur Wägung dünner Schichten und zur Mikrowägung," Zeitschrift für Physik, 155, 206-222 (1959)

[4] P. Lostis, "Étude, réalisation et contrôle de lames minces introduisant une différence de marche déterminée entre deux vibrations rectangulaires," Part 2: "Nouvelle méthode de contrôle de l'epaisseur pendant l'évaporation," Revue d'optique, théorique et instrumentale, 38, 1-28 (1959)

[5] E. Benes, "Improved quartz crystal microbalance technique," J. Appl. Phys., 56, 608-626 (1984)

[6] H. Nowotny and E. Benes, "General one-dimensional treatment of the layered piezoelectric resonator with two electrodes," J. Acoust. Soc. Am., 82, 513-521 (1987)

[7] A. Ballato, "Compound resonators and microweighing sensors," IEEE Intl. Frequency Contr. Symp. Proc., 186-191 (2006)

[8] W. P. Mason, "Measurement of the viscosity and shear elasticity of liquids by means of a torsionally vibrating crystal," Trans. Am. Soc. Mech. Eng., 68, 359-370 (1947)

[9] W. P. Mason, "Viscosity and shear elasticity measurements of liquids by means of shear vibrating crystals," J. Colloid Sci. 3, 147-162 (1948)

[10] W. P. Mason, W. O. Baker, H. J. McSkimin, J. H. Heiss, "Measurement of shear elasticity and viscosity of liquids at ultrasonic frequencies," Phys. Rev., 75, 936-946 (1949)

[11] E. F. Carome and R. P. Moeller, "An improved viscometer for studies of simple fluids in the critical region," IEEE Ultrasonics Symp. Proc., pp. 109-111, Boston, MA, October 1972. Abstract: IEEE Transactions on Sonics and Ultrasonics, vol. SU-20, no. 1, p. 43, paper A-6, January 1973.

[12] Z. Kojro, E.v.d. Burg, J. Zinke, K. Hillmann, W. Grill, "Viscosity shear waves and mass drag effects in liquids," Zeitschrift für Physik B 101, 433-439 (1996)

[13] Y. Kim, J. R. Vig, A. Ballato, "Sensing the properties of liquids with doubly rotated resonators," IEEE Intl. Freq. Contr. Symp. Proc., 660-666 (1998)

[14] A. Ballato, "Piezoelectric resonators loaded with viscoelastic and nonuniform media," IEEE Intl. Freq. Contr. Symp. Proc., 191-201 (2002)

[15] E. Benes, R. Thalhammer, M. Gröschl, H. Nowotny, S. Jary, "Viscosity sensor based on a symmetric dual quartz thickness shear resonator," IEEE Intl. Frequency Contr. Symp. & 17th Eur. Freq. and Time Forum Proc., 1048-1054 (2003)

[16] D. C. Ash, M. J. Joyce, C. Barnes, C. J. Booth, A. C. Jefferies, "Viscosity measurement of industrial oils using the droplet quartz crystal microbalance," Meas. Sci. Technol. 14, 1955-1962 (2003)

[17] A. Saluja, D. S. Kalonia, "Measurement of fluid viscosity at microliter volumes using quartz impedance analysis," AAPS PharmSciTech, 5, Art. 47 (2004)

[18] Y. Kim, J. R. Vig, A. Ballato, "Doubly rotated resonators for sensing the properties of liquids," IEEE Trans. Ultrason., Ferroelect., Freq. Contr. 51, 1388-1393 (2004)

[19] C. D. Stockbridge, "Effects of gas pressure on quartz-crystal microbalances," in Vacuum Microbalance Techniques, 5, 147-178 Plenum (1966)

[20] C. D. Stockbridge, "Effect of hydrostatic pressure on rotated Y-cut quartz crystal resonators," in Vacuum Microbalance Techniques, 5, 179-191 Plenum (1966)

[21] A. Ballato, "Resonance in piezoelectric vibrators," Proc. IEEE 58, 149-151 (1970)

[22] D. W. Dye, "The piezo-electric quartz resonator and its equivalent electrical circuit," Proc. Phys. Soc. (London), 38, 399-458 (1926)

[23] R. W. Cernosek, S. J. Martin, A. R. Hillman, H. L. Bandey, "Comparison of lumped-element and transmission-line models for thickness-shear-mode quartz resonator sensors," IEEE Intl. Freq. Contr. Symp. Proc., 96-104 (1997)

[24] A. Ballato, "Modeling piezoelectric and piezomagnetic devices and structures via equivalent networks," IEEE Trans. Ultrason., Ferroelect., Freq. Contr. 48, 1189-1240 (2001)

[25] U. Hempel, R. Lucklum, P. R. Haupmann, E. P. EerNisse, D. Puccio, R. F. Diaz, "Quartz crystal resonator sensors under lateral field excitation – A theoretical and experimental analysis," Meas. Sci. Technol. 19, art. 055201 (2008)

[26] J. W. S. Rayleigh, The Theory of Sound, Vol. 2, 2nd revised edition, (1896), Dover, New York (1945)

[27] P. E. Tenzer, R. B. Mrad, "A systematic procedure for the design of piezoelectric inchworm precision positioners," IEEE/ASME Trans. Mechatronics, 9, 427-435 (2004)

[28] J. Hilsenrath, C. W. Beckett, W. S. Benedict, L. Fano, H. L. Hoge, J. F. Masi, R. L. Nuttall, Y. S. Touloukian, and H. W. Woolley, "Tables of Thermal Properties of Gases," NBS Circular 564, National Bureau of Standards, Washington, DC (1955)

[29] J. Hilsenrath, "Thermodynamic Properties of Gases," in American Institute of Physics Handbook, 2nd ed., D. E. Gray, Ed., McGraw-Hill, New York (1963)

[30] N. J. Themelis, *Transport and Chemical Rate Phenomena*, Gordon and Breach, Basel, 1995.

[31] M. Levy, H. E. Bass, and R. Stern, Eds., *Handbook of Elastic Properties of Solids, Liquids, and Gases*, Academic Press, San Diego, CA, 2001. Vol. IV, Elastic Properties of Fluids: Liquids and Gases. ISBN: 0-12-445764-9.